Trans Indian Inst Met (2018) 71(11):2759–2763
https://doi.org/10.1007/s12666-018-1447-0

TECHNICAL PAPER

Grain Refinement of B319 Alloy Using Spark Plasma Sintered Al–Ti–C Grain Refiners

Anil Prasad[1] · Justin Mok[1] · Levi Lafortune[1] · Lukas Bichler[1]

Received: 15 July 2018 / Accepted: 18 September 2018 / Published online: 3 October 2018

Abstract The B319 aluminum alloy is a candidate material for automotive applications, where engineers and material designers are seeking to improve vehicle efficiency through vehicle weight reduction. Although the alloy has many desirable properties, such as excellent castability and moderate strength-to-weight ratio, efforts to further enhance the alloy's strength via the grain refinement approach play a key role to a wider adaptation of the alloy. However, there remain challenges related to the efficient dispersion of inoculating particles in the liquid alloy during casting. The present research has focused on examining the grain refining ability of various novel grain refiners produced via the spark plasma sintering powder metallurgy process. Two novel grain refiners [aluminum–titanium carbide (Al–TiC) and aluminum–titanium–carbon black (Al–Ti–C_b)] were produced at high and low concentrations and then added to the molten B319 alloy. The grain refiners got dispersed within the melt, thus overcoming the need for external melt stirring or treatment. The high concentration formulations for both Al–TiC and Al–Ti–C_b achieved a reduction in the average grain size by 31% and 25%, respectively.

✉ Lukas Bichler
lukas.bichler@ubc.ca

Anil Prasad
anil@alumni.ubc.ca

Justin Mok
justinmok4@gmail.com

Levi Lafortune
levi.laf@gmail.com

[1] School of Engineering, University of British Columbia Okanagan, Kelowna, Canada

Keywords Spark plasma sintering · B319 · Grain refinement · Al–TiC

1 Introduction

Aluminum–copper (Al–Cu) alloys are commonly used in automobile and aerospace applications due to their low density and precipitation hardenability [1, 2]. The B319 aluminum alloy is a commercially available Al–Si–Cu–Mg alloy with 5.5–6.5 wt% Si, 4.0–5.0 wt% Cu, 1.2 wt% Fe, 0.1–0.5 wt% Mg, 0.8 wt% Mn, 0.5 wt% Ni, 1.0 wt% Zn, 0.5 wt% Ti and balance Al. Typically, Si is added to Al–Cu alloys to lower the melting point and thus improve castability [3]. Mg is added to facilitate the formation of more complex hardening phases, such as the Mg_2Si and $Al_5Cu_2Mg_8Si_6$ [4]. Zn is added to the B319 alloy to enhance precipitation hardening during heat treatment [4, 5], while Mn is added to improve the tensile strength, fatigue resistance and corrosion resistance [5]. Fe forms intermetallic precipitates with Al and Mn, which further enhances mechanical properties [5]. Ni and Ti are added to the alloy to enhance creep resistance and grain refinement, respectively [5].

Although heat treatment and precipitation hardening can be used for microstructure modification and property enhancement, these treatments may lead to casting dimensional distortion and non-uniform microstructure in the case of complex 3D castings. In the case of as-cast alloys, grain refinement may achieve comparable results [6], since the addition of grain refiner particles create heterogeneous nucleation sites, which promote finer grain size, dispersed second phases and enhancement of mechanical properties in the as-cast material [7].

Current grain refinement techniques often rely on the addition of grain refiner particles to the liquid alloy via a

master alloy [8–10]. For example, an Al–Ti–B master alloy prepared by mixing KBF_4 and K_2TiF_6 salts in molten aluminum metal is found to be effective in treating aluminum alloys; however, the master alloys often introduce unreacted salts, porosity and chemical inhomogeneity into the final casting [10, 11]. In case of Al alloys, Al–Ti–B and Al–Ti–C are commonly used grain refiners [12]; however, it has been found that the presence of TiB_2 is detrimental for the formability and electrical conductivity of as-cast materials [13]. In addition, the TiB_2 and AlB_2 particles present in the grain refiner are susceptible to poisoning and fading effects, respectively [12]. Vinod Kumar et al. [14] reported that lower addition of Al–Ti–C grain refiners might achieve comparable results to Al–Ti–B. In an earlier publication, the same research group had also shown that TiB_2 particles showed tendency to settle in comparison with TiC particles [15]. An investigation by Ding et al. [16] demonstrated that the Al–Ti–C grain refiner had a better grain refining ability than the Al–Ti or Al–TiC refiners. Prior work by Kumar et al. [8] revealed that addition of 0.03 wt% TiC to the final alloy was most effective for grain refining.

Spark plasma sintering (SPS) is a novel sintering technique that has been researched widely for sintering fully dense ceramic, metallic and composite pellets [17–19]. Recent studies have applied SPS technique for the fabrication of a wide variety of grain refiner master alloys [20–24].

In this study, Al–Ti–C-based master alloys were prepared using SPS and used to grain refine the B319 alloy. Two master alloys were examined: Al–TiC (aluminum–titanium carbide) and Al–Ti–C_b (aluminum–titanium–carbon). The carbon used in this study was in the form of a carbon black powder, which is an amorphous allotrope of carbon. Two concentration levels of these grain refiners were examined to study their effect on the grain refining potency. A comparison between refined and unrefined alloys was drawn using microstructure analysis, fluidity, hardness test and scanning electron microscopy (SEM). The results were also compared to a B319 alloy treated with pure TiC powder particles.

2 Experimental Procedure

A detailed experimental procedure pertaining to the research has been published elsewhere [20]. All raw powders used for the grain refiners had a purity of at least 99.5%. The master alloy blends were prepared by mixing precursor powders in a planetary ball mill in ethanol. After drying, the powder blends were sintered using an SPS machine. Two different compositions of master alloys were sintered to study the impact of grain refiner concentration on the B319 alloy's microstructure. Also, a pellet made of pure Al (i.e., no additives) was sintered.

1. Al–1TiC (1 wt% TiC, bal. Al)
2. Al–5TiC (5 wt% TiC, bal. Al)
3. Al–1(Ti–C_b) (0.9 wt% Ti, 0.1 wt% C_b, bal. Al)
4. Al–5(Ti–C_b) (3.6 wt% Ti, 0.4 wt% C_b, bal. Al)
5. TiC: 0.03 wt% TiC loose powder was added by wrapping in Al foil.

Casting experiments were carried out with two molds. The first mold was a cylindrical graphite mold with 25.4 mm ID and a length of 102 mm. This graphite mold was wrapped in a heating tape and an alumina blanket and preheated to 350 °C. The B319 alloy was heated to 710 °C, when the grain refiner was added and stirred for 30 s before making a pour. The amount of master alloy added to the B319 aluminum alloy was calculated such that the total grain refiner addition to the alloy was 0.03 wt%. A casting cross section was polished to perform hardness tests and microstructure evaluation.

A second mold was also fabricated to study the effect of the grain refiners on the B319 alloy's fluidity. A spiral mold made of mild steel with a fluidity spiral cavity [25, 26] was preheated to 300 °C, and the same B319 alloy treatment with grain refiners was followed for fluidity tests.

The samples were etched with Keller's reagent prior to grain size measurements. To obtain statistically significant grain size measurement, the linear intercept method was used on a minimum of 50 random locations. A Tescan Mira3 SEM with Oxford EDS attachment was used for microscopy and chemical analyses. A Brinell hardness tester was used to determine the as-cast alloy hardness.

3 Results and Discussion

3.1 Characterization of Ingots and Master Alloys

The as-sintered Al–TiC and Al–Ti–C_b master alloys had a density of 97.5% and 97%, respectively. A pure aluminum pellet sintered under the same condition had a density of 98%. Hence, the addition of the grain refiner particles had a negligible effect on the sinterability of the master alloys. Figure 1 shows the SEM microstructure of the as-sintered master alloys. In general, the microstructure comprised of the additive (TiC, Ti and C_b) particles distributed along the boundaries of the aluminum matrix particles throughout the entire pellet. The bright particles in Fig. 1a represented the TiC particles (the image in the inset represents a higher magnification view). The sintered Al–5Ti–C_b pellet had three different regions distinctly visible in the micrograph: (1) gray Al matrix, (2) bright Ti particles and (3) dark C particles. The inset image shows the C_b-rich region.

Figure 2 shows the optical macrographs of the etched alloy samples. In the case of the unrefined B319 alloy, the grains were large and visible with naked eye. There was no

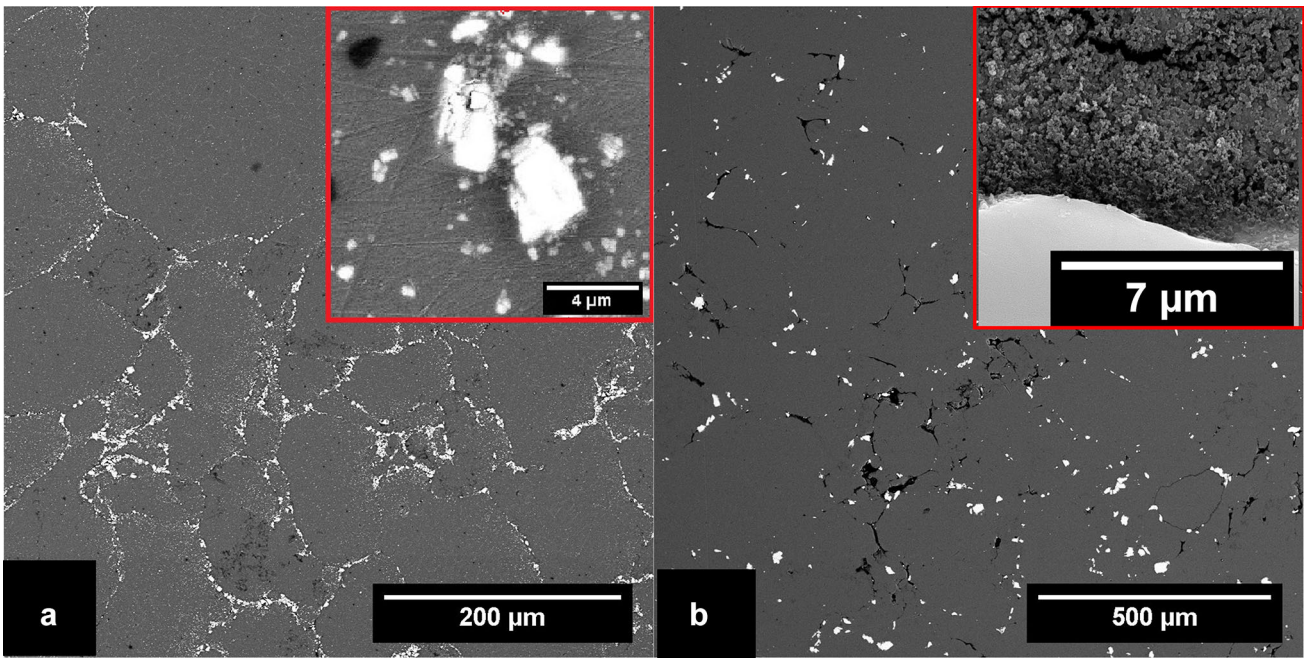

Fig. 1 BSE images of as-sintered master alloys **a** Al–5TiC (inset: TiC particles), **b** Al–5(Ti–C_b) (inset: C_b particles)

statistically significant difference in the grain size between the unrefined alloy and the alloy refined with pure TiC loose powder. However, as seen in Fig. 2, a noticeable decrease in grain size in the alloys refined with SPS master alloys were observed. Figure 3 shows the result of image analysis of grain size measurement. The average grain size for unrefined alloys was ~ 2500 µm. There was a slight decrease in the average grain size when a TiC lose powder was added to the B319 alloy. However, when SPS prepared master alloys were added, the grain size significantly

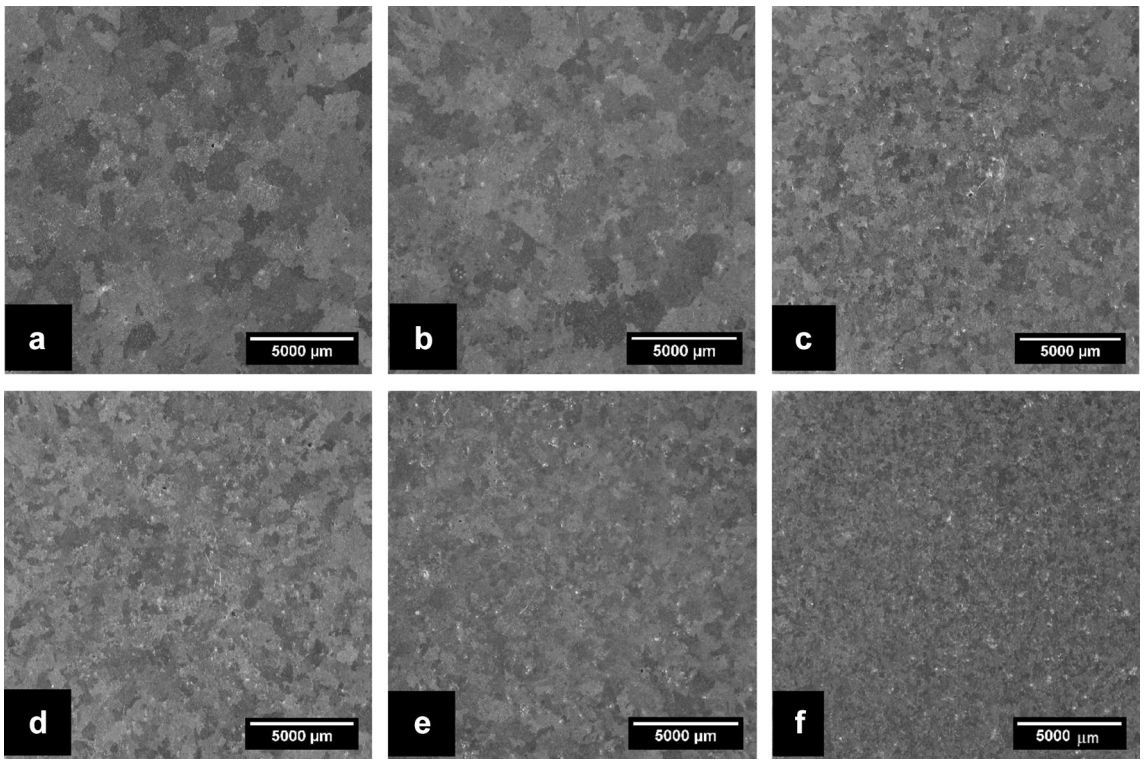

Fig. 2 Grain structure of as-cast B319 alloy samples **a** unrefined, **b** TiC powder, **c** Al–1TiC, **d** Al–5TiC, **e** Al–1(Ti–C_b), **f** Al–5(Ti–C_b)

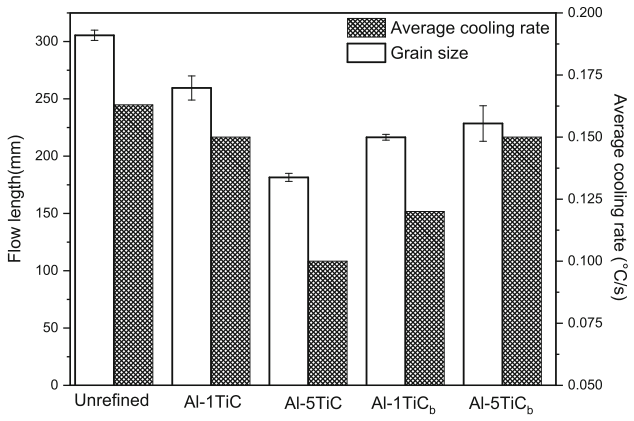

Fig. 3 Box plots of grain sizes of unrefined and refined alloys superimposed above bar chart of averaged grain size from both trials

reduced to: Al–1TiC (1030 µm) and Al–5TiC (720 µm). A further decrease in grain size was observed for castings treated with carbon black containing master alloys: Al–1(Ti–C_b) (850 µm) and Al–5(Ti–C_b) (540 µm). The inferior grain refinement with the TiC particles was likely the result of their tendency to agglomerate due to their larger size. In all casting trials with SPSed master alloys, the additive particles were uniformly distributed in the master alloy, thus providing ample nucleation sites resulting in a finer grain size. The difference in grain size between the high concentration and low concentration grain refiners was statistically insignificant. Although the change in the grain size between the Al–TiC and Al–Ti–C_b grain refiners was relatively small, Fig. 4 shows that the Ti particles in the B319 alloy after addition of Al–5(Ti–C_b) enabled the formation of a new phase in the vicinity of the Ti particles. An EDS linescan identified this phase was found to have an approximate stoichiometry matching that of $TiAl_3$. Such a grain refinement mechanism has been reported in the literature and plays a critical role in grain refinement by Al–Ti-based master alloys [22, 23].

3.1.1 Hardness

The HR15T hardness values were plotted in Fig. 5a. There was a clear increase in the alloy hardness with the grain refiner addition. The B319 alloy with addition of Al–TiC and B319 alloy with Al–Ti–C_b had a higher hardness than the B319 alloy with TiC loose powder-treated alloys (or the pure B319 alloy). Additionally, there was an increase in the hardness with increase in grain refiner concentration. The increase in hardness values correlated well to the grain size dependency, as governed by the Hall–Petch relationship, since the hardness values were directly proportional to $1/(grainsize)^{1/2}$, as shown in Fig. 5a.

3.1.2 Fluidity Testing

As shown in the graph in Fig. 5b, the unrefined alloy had the highest flow length of all alloy compositions investigated. In the of the Al–TiC-treated castings, the fluidity decreased with increasing concentration of the grain refiner. However, in case of the Al–Ti–C_b alloys, there was no

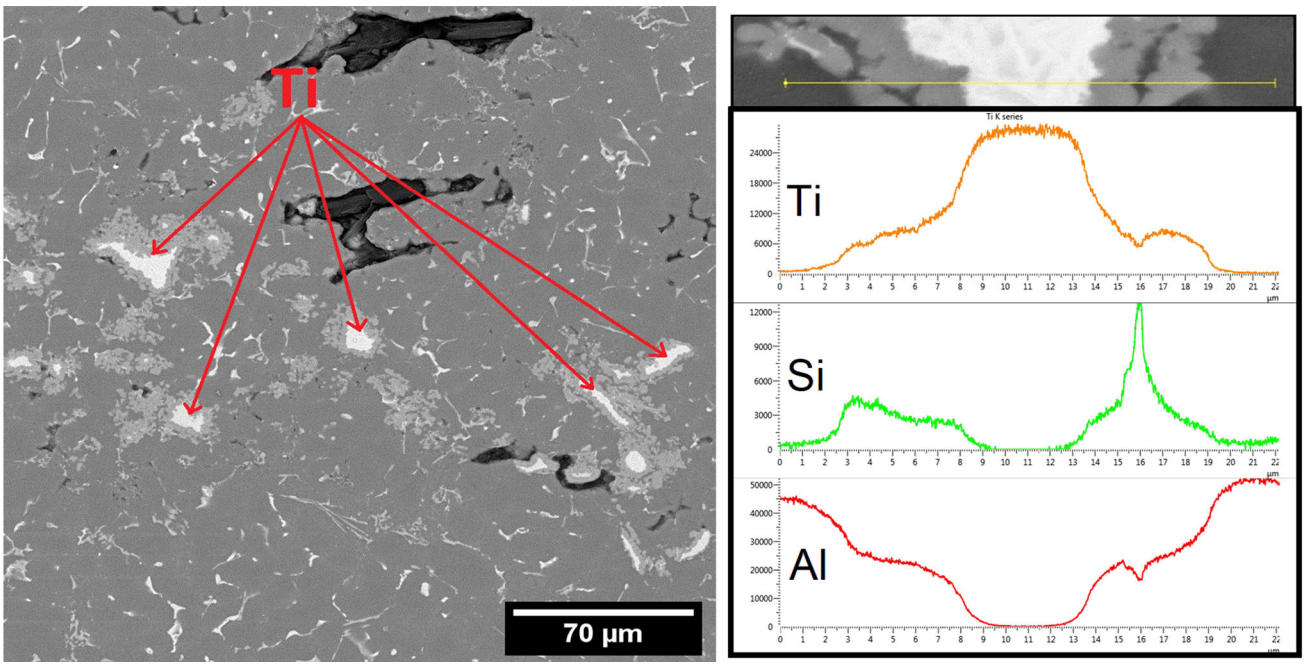

Fig. 4 BSE image of Ti grain refiner particles with $TiAl_3$ phase surrounding it in Al–5(Ti–C_b) alloy

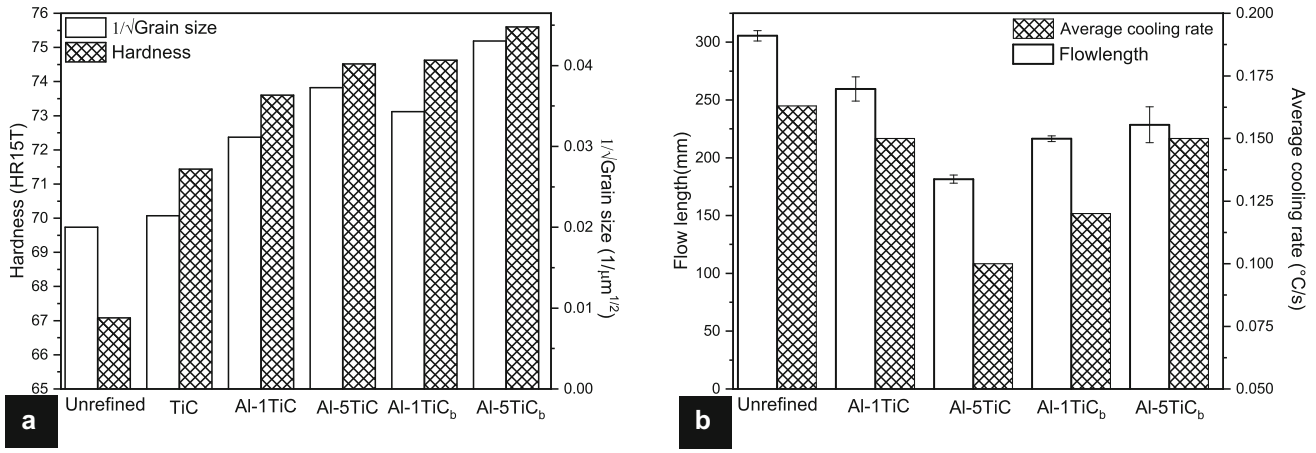

Fig. 5 **a** Hardness values plotted alongside reciprocal of grain size values. **b** Flow length of unrefined and refined alloys

clear correlation between the grain refiner's concentration and the alloy fluidity.

The average cooling rate of the casting was calculated using the temperature recorded at 104 mm of the flow length in the spiral mold. A higher cooling rate enabled faster fraction of solid evolution, which would increase the melt viscosity. However, there were few reports that suggested that casting issues, such as oxide formation, turbulence and local heat transfer conditions, might have a significant impact on alloy fluidity [25, 26].

4 Conclusion

The following conclusions were drawn from this study

1. The Spark Plasma Sintering process enabled fabrication of a grain refiner with uniformly dispersed reinforcing particles.
2. The TiC powder addition seemed to have aided in grain refinement by decreasing the grain size from 2500 to 2180 μm. This is in accordance with past literature.
3. The alloys treated with grain refiners manufactured by SPS exhibited a significant grain size reduction.
4. Also there was a clear correlation between grain refiner concentration and grain sizes. A higher grain size concentration implied a finer grain size, probably due to increase in nucleation sites.
5. The hardness values followed a Hall–Petch relation with grain size variation.

References

1. Starke E, and Staley J, *Prog Aerosp Sci* **32** (1996) 131.
2. Davis J R, *Aluminum and Aluminum Alloys*, ASM International, Russell Towns (1993) 355.
3. Kalhapure M G, and Dighe P M, *Int J Sci Res* **6** (2013) **38**.
4. Samuel A, Doty H, Valtierra S, and Samuel F, *Mater Des* **52** (2013) **2457**.
5. -Yan L, Zhang Y, Li X, Li Z, Wang F, Liu H, and Xiong B, *Prog Nat Sci Mater Int* **24** (2014) 97.
6. Guan R-G, and Tie D, *Acta Metall Sin (Engl Lett)* **30** (2017) 409.
7. Malekan M, and Shabestari S, *Metall Mater Trans A* **40** (2009) 3196.
8. Kumar V, and Bichler L, *Trans Indian Inst Metals* **68** (2015) 1173.
9. Birol Y, *Materials* **7** (2014) 1749.
10. Toptan F, Kerti I, Dablilar S, Sagin A, Karadeniz O F, and Ambarkutuk A, *Light Met* 2011, Springer, Cham (2011) 821.
11. Birol Y, *J Alloys Compounds* **458** (2008) 271.
12. Murty B S, Kori S A, and Chakraborty M, *Int Mater Rev* **47** (2002) 3.
13. Lafortune L, MASc Thesis, University of British Columbia Okanagan, Canada.
14. Vinod Kumar G S, Murty B S, Chakraborty M, *J Alloy Compounds* **472** (2009) 112.
15. Vinod Kumar G S, Murty B S, and Chakraborty M, *J Alloy Compounds* **396** (2005) 143.
16. Ding W, Zhu J, Zhao W, and Xia T, *Adv Metals Res* **652** (2013) 1072.
17. Schwertz M, Lemonnier S, Barraud E, Carradò A, Vallat M-F, and Nardin M, *Powder Metall* **58** (2015) 87.
18. Shen Z, Johnsson M, Zhao Z, and Nygren M, *J Am Ceram Soc* **85** (2002) 1921.
19. Anselmi-Tamburini U, Garay J, and Munir Z, *Scr Mater* **54** (2006) 823.
20. Mok J, *Grain Refinement of B319 Alloy Using Spark Plasma Sintered Al–Ti–C Grain Refiners*, MASc Thesis, University of British Columbia, Canada.
21. Davis T, Bichler L, D'Elia F, and Hort N, *J Alloy Compounds* **759** (2018) 70.
22. Azad A, Bichler L, Elsayed A, *Int J Metalcasting* **7** (2013) 49.
23. Davis T, Bichler L, D'Elia F, and Hort N, *Magnesium Technology 2017*, The Minerals, Metals & Materials Series. Springer, Cham (2017) 653.
24. Davis T, Bichler L, Sediako D, and Balogh L, *Magnesium Technology 2018*, The Minerals, Metals & Materials Series. Springer, Cham (2018) 425
25. Turen Y, *Mater Des* **49** (2013) 1009.
26. Behera R, Chatterjee D, and Sutradhar G, *Am J Mater Sci* **2** (2012) 53.